J. Appl. Cryst. (1996). **29**, 419–426

Electron Diffraction Patterns of Fibrous and Lamellar Textured Polycrystalline Thin Films. II. Applications

L. TANG, Y. C. FENG, L.-L. LEE AND D. E. LAUGHLIN

Data Storage Systems Center, Department of Materials Science and Engineering, Carnegie Mellon University, Pittsburgh, PA 15213, USA

(*Received 20 October 1995; accepted 8 January 1996*)

Abstract

Electron diffraction patterns of a sputter-deposited polycrystalline MgO thin film on an SiO_2 substrate, of a Ta thin film and of CoCrTa/Cr bilayer films on glass substrates are presented and analyzed based on the theory developed in Paper I [Tang & Laughlin (1996). *J. Appl. Cryst.* **29**, 411–418]. It is found that the MgO film is [001] textured with a distribution angle of 13°. The Ta film is composed both of randomly oriented grains and [011] textured grains. The [011] texture axis distribution angle of the Ta film is determined to be 11°. $(11\bar{2}0)$CoCrTa/(001)Cr and $(10\bar{1}1)$CoCrTa/(011)Cr polycrystalline epitaxy are identified in the CoCrTa/Cr bilayer films. Both the bilayer films have a texture axis distribution angle of 6°.

1. Introduction

Polycrystalline monolayered and multilayered thin films deposited on substrates are under intensive investigation for various applications. In most cases, a certain texture for a single layered film and a certain epitaxial relationship between grains of different layers in a multilayered film are required in order to achieve the desired properties. Thus, polycrystalline thin-film texture and epitaxy analysis is essential for optimization and understanding of the mechanisms of the novel properties achieved in many systems. In this paper, we present the results of electron diffraction investigations on the textures of MgO/SiO_2 and Ta/glass and the epitaxial relationship of CoCrTa/Cr bilayers deposited on glass substrates, on the basis of the theory developed in paper I (Tang & Laughlin, 1996).

2. Experimental

Single-layer MgO and Ta films as well as $CoCr_{12}Ta_2$/Cr bilayer films used in this study were RF-diode-sputter-deposited on oxidized (100) Si or glass substrates using a Leybold–Heraeus HZ-400 sputtering system. The base vacuum was approximately 7×10^{-5} Pa. Table 1 summarizes the thickness and sputter deposition parameters of the films. Transmission electron microscopy (TEM) specimens were prepared by mechanical grinding, dimpling and Ar^+ ion-milling from the substrate side. The microstructure, texture and epitaxy studies of the films were then carried out using a 120 kV Philips 420-T transmission electron microscope with a $\pm 60°$ goniometer.

3. Results and discussion

3.1. *[001] textured MgO film*

MgO has the NaCl structure ($B1$, $Fm\bar{3}m$) with a lattice parameter of $a = 4.21$ Å (JCPDS Diffraction Data Card, 1992). Fig. 1 is a bright-field image of the MgO film at 0° tilt, *i.e.* the normal to the film is parallel to the incident electron beam. The grain size estimated from this micrograph is about 40 nm. It can be noted that there are many grains in dark contrast, *i.e.* oriented at strong diffraction conditions. This indicates that the film has a crystallographic texture. Fig. 2(*a*) shows the corresponding diffraction pattern of the film at 0° tilt, which has been defined as the *parallel pattern* in paper I. The observed rings in this parallel pattern are 200_0, 220_0, 400_0 and 420_0. No 111_0 or 311_0 rings are observed. This is consistent with the film having a [001] texture, as can be seen from equation (7) in paper I (Tang & Laughlin, 1996). The intensity ratios of the rings in the parallel pattern also agree with those calculated for a [001] textured MgO film. These are listed in Table 2, together with the intensity ratios of a randomly oriented MgO film. Also in Table 2 are the d spacings, structure factors (for 120 kV electrons) and multiplicity factors P for the various hkl planes in both cases. It should be pointed out that the intensity ratios of the rings for a film with randomly oriented grains do not change when the specimen is tilted. Also, no diffraction arcs would be formed for random films during specimen tilting. As discussed in paper I, the hkl_i arcs, $i = 1, 2, \ldots, N$ or $N-1$, where N is the number of distinct angles of the $\{hkl\}$ with the texture axis, always appear first as single arcs along the axis **OF** at a tilt angle $\beta_i^s = 90° - \eta_i - \alpha$. These single arcs eventually split into a pair of arcs after further tilting

Table 1. *Deposition conditions and thicknesses of the films*

Thin film	Substrate	Substrate temperature (K)	Substrate bias (V)	Ar gas pressure (Pa)
MgO (1000 Å)	Oxidized (100) Si	Room	0	1.3
Ta (1000 Å)	Glass	823	0	1.3
CoCrTa/Cr (200/1000 Å)	Glass	533	0	1.3
CoCrTa/Cr (400/1000 Å)	Glass	423	−150/−200	1.3

by 2α, to the tilt angle $\beta_i^e = 90° - \eta_i + \alpha$. Here, η_i is the angle between hkl_i and the texture axis and α is the texture axis distribution angle. The axis **OF** is perpendicular to the tilt axis **OT**, which always bisects the hkl_0 arcs.

The conclusion that the MgO film is [001] textured can be further confirmed by the diffraction patterns taken after the film is tilted about the axis **OT** in the film plane. Figs. 2(*b*)–(*f*) show the diffraction patterns of the film at 30, 36, 46, 51 and 60° tilt with the tilt axis **OT** and axis **OF** also drawn in Fig. 2(*b*). Figure 3 is the 60° tilt pattern indexed using the method described in paper I. Since the four planes of the {111} family of a face-centered cubic (f.c.c.) lattice make only one distinct angle, $\eta_1 = 54.7°$, with the [001] axis (see Table 1 of paper I), the 111_1 diffraction arcs should appear in the diffraction pattern after the specimen is tilted by $\beta_1^s = 90 - \eta_1 - \alpha = 35.3° - \alpha$ for a [001] textured film. Similarly, the tilt angles at which the 200_1, 220_1, 400_1, 311_1 and 311_2 diffraction arcs are first observed are $90° - \alpha$, $45° - \alpha$, $90° - \alpha$, $17.5° - \alpha$ and $64.8° - \alpha$, respectively. Indeed, the diffraction patterns closely follow these predictions in the tilt angle range 0–60° of the experiment. The 111_1 arc was first observed to appear along the **OF** axis after about 20° tilt and then split into two arcs at about 50° tilt (Fig. 2*e*). This indicates that α is about 15° for this specimen. This value of α is also determined from the 220_1 arc, which first appears at about 30° tilt and splits into two arcs after about a 60° tilt.

From Figs. 2 and 3, we note that the angle ω_0 subtended by the hkl_0 arcs, *i.e.* 200_0, 220_0, 400_0 and 420_0, decreases with increase of the tilt angle β. There are no 110_0 or 311_0 arcs along **OT**. It can also be seen that the angle ω_{111_1} subtended by the unsplit 111_1 arc increases with the tilt angle (Figs. 2*b*, *c* and *d*) until it splits into two arcs (Fig. 2*e*). This is also true for the unsplit 220_1 arc (Figs. 2*b*, *c*, *d* and *e*). As pointed out in paper I, the α value can also be determined from the plots of $\sin(\omega_0/2)$ *vs* $1/\sin\beta$ and $\cos(\omega_{hkl_i}/2)$ *vs* $1/\sin\beta$ by the following relations:

$$\sin(\omega_0/2) = \sin\alpha/\sin\beta \quad \alpha \le \beta \le 90°; \tag{1}$$

$$\cos(\omega_{hkl_i}/2) = \sin\beta_i^s/\sin\beta$$
$$i = 1, 2, \ldots, N \quad \text{or} \quad N-1, \quad \beta_i^s \le \beta \le \beta_i^e. \tag{2}$$

Here, ω_{hkl_i} is the angle subtended by the unsplit hkl_i arc along **OF**. Fig. 4 is the $\sin(\omega_0/2)$ *vs* $1/\sin\beta$ plot for the film. The distribution angle α is determined to be 14° from the slope of the best-fit straight line. Figs. 5 and 6

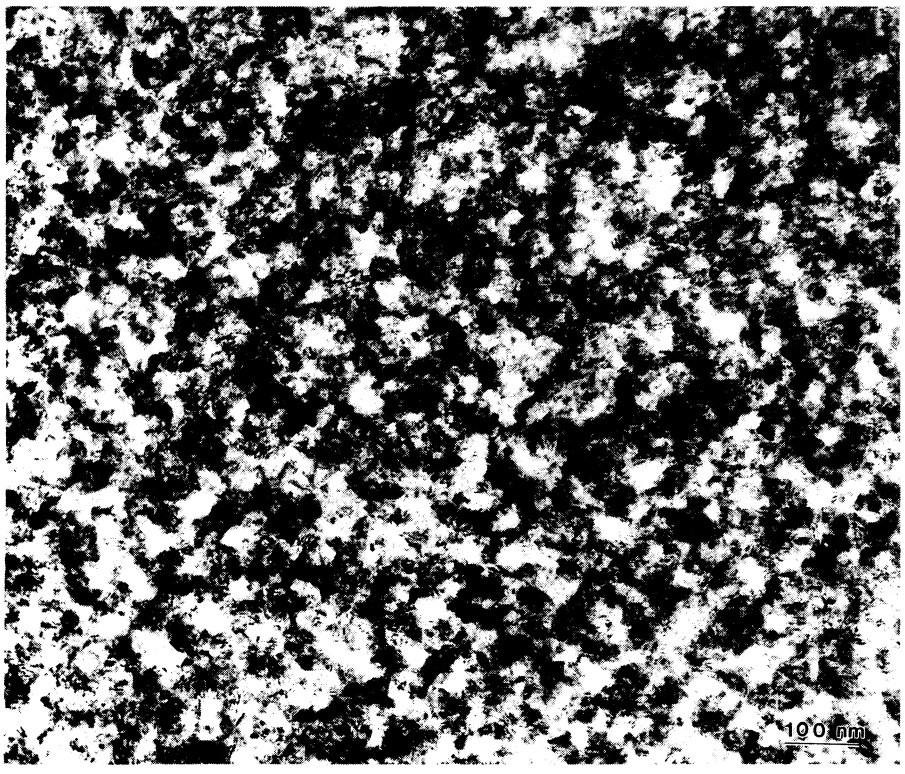

Fig. 1. Bright-field TEM image of the [001] textured MgO film at 0° tilt.

Table 2. *Crystallographic parameters and calculated intensity ratios of parallel electron diffraction rings for randomly oriented and [001] textured grains of MgO films*

hkl	d (Å)	F (Å)	P_r	I_r	$P_{[001]}$	$I_{[001]}$
111	2.43	2.48	8	5	0	0
200	2.11	14.24	6	100	4	100
220	1.49	9.84	12	48	4	24
311	1.27	0.60	24	3	0	0
222	1.22	7.75	8	13	0	0
400	1.05	6.44	6	5	4	5
331	0.97	0.64	24	2	0	0
420	0.94	5.55	24	12	4	3
422	0.86	4.85	24	8	0	0

are the $\cos(\omega_{111_1}/2)$ *vs* $1/\sin\beta$ and $\cos(\omega_{220_1}/2)$ *vs* $1/\sin\beta$ plots for the film. The α values determined from the slope [*i.e.* $\sin(35.3^\circ - \alpha)$ for the 111_1 arc and $\sin(45^\circ - \alpha)$ for the 220_1 arc] of the best-fit straight lines of Figs. 5 and 6 are 12 and 13°, respectively. These values of α determined from Figs. 4, 5 and 6 agree well with the α value determined directly from measurements of β_1^s and β_1^e of the 111_1 and 220_1 arcs (*i.e.* 15). Assuming we can detect intensity 10% over background and a Gaussian distribution of the texture axis, can show that our α value is approximately 1.75 times larger than the $\Delta\theta_{50}$ value measured by the X-ray rocking-curve technique.

3.2. *[011] textured Ta film*

Thin films of Ta have been reported to have either a body-centered-cubic (b.c.c.) ($a = 3.303$ Å) structure or a tetragonal ($a = 5.34$, $c = 9.94$ Å) structure (Read & Altman, 1965; Read & Hensler, 1972). The Ta film investigated in this study has a grain size of about 15 nm (Fig. 7) and displays a b.c.c. structure as can be seen from its 0° tilt diffraction pattern (Fig. 8*a*). In Fig. 8(*a*), all the allowed b.c.c. rings (*i.e.* $h+k+l=$ even) are observed. The intensity ratios of the rings, however, are different

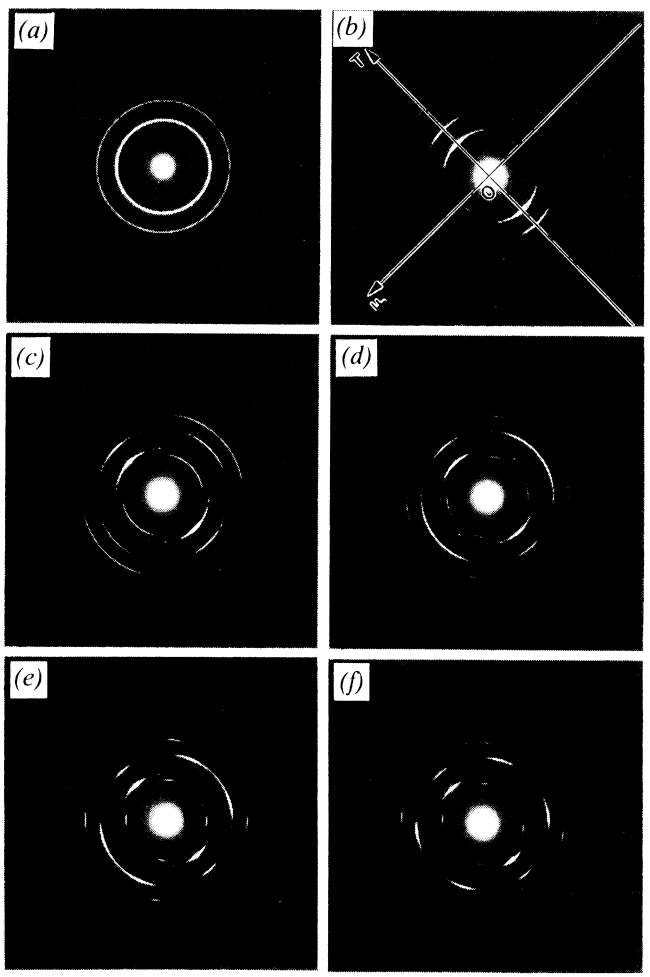

Fig. 2. Electron diffraction patterns of the [001] textured MgO film at (*a*) 0, (*b*) 30, (*c*) 36, (*d*) 46, (*e*) 51 and (*f*) 60° tilt.

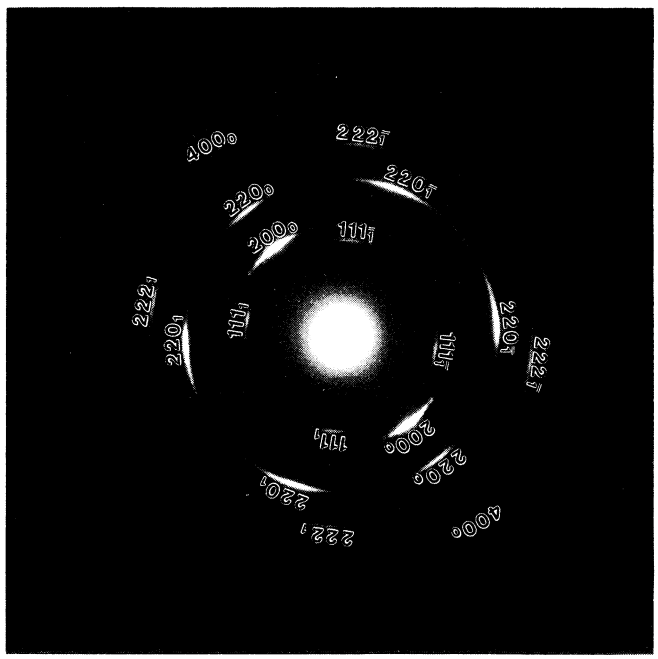

Fig. 3. Indexed electron diffraction pattern of the [001] textured MgO film at 60° tilt.

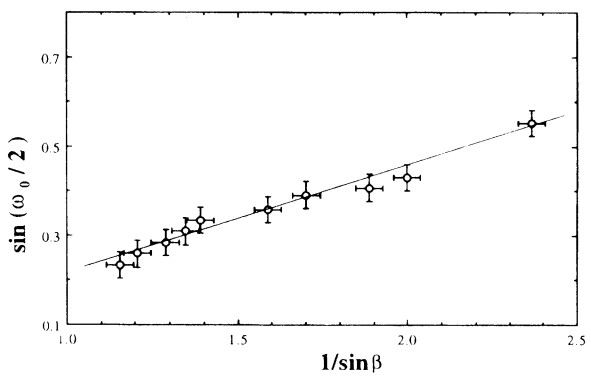

Fig. 4. $\sin(\omega_0/2)$ *vs* $1/\sin\beta$ plot of the [001] textured MgO film.

from those calculated for randomly oriented grains. This can be seen from Table 3, in which the intensity ratios of diffraction rings for the randomly oriented and for the [011] textured Ta film at 0° tilt are listed together with d spacings, structure factors (for 120 kV electrons), and multiplicity factors for both cases. Note that the 222 ring is stronger than the 310 and 321 rings. Thus, the film is partially textured. The fact that the intensities of the 200 and 211 rings are nearly the same and the 310 and 321 rings are weak in Fig. 8(a) indicates that the film is [011] textured (for an ideally [011] textured b.c.c. film there would be no 310_0 and 321_0 rings in the parallel pattern) (see Table 3). Since the six planes of the {110} family of a cubic lattice make three distinct angles (0, 60 and 90°) with the [011] axis (see Table 1 of paper I), we would expect to observe the 110_0 arcs along the tilt axis when $\beta \geq \alpha$ and the 110_1 arc when $\beta \geq 30 - \alpha$, as well as the 110_2 arc when $\beta \geq 90 - \alpha$ along **OF** if the film has the [011] texture. Similarly, the three planes of the {200} family have two distinct angles (45 and 90°) with the [011] axis and, therefore, the 200_1 arc will start appearing at $45° - \alpha$ tilt in addition to 200_0 arcs along **OT** after $\beta \geq \alpha$. For the twelve planes of the {211} family, there are four distinct angles (30, 54.73, 73.22 and 90°) with the [011] direction. Therefore, in addition to the 211_0 arcs along the tilt axis when $\beta \geq \alpha$, the 211_1, 211_2 and 211_3 arcs will be observed after tilting to angles of $16.78° - \alpha$, $35.27° - \alpha$ and $60° - \alpha$. The diffraction patterns of the Ta film at tilt angles of $\beta = 23$, 32, 38, 46 and 54° are shown in Figs. 8(b)–(f). Fig. 9 is the indexed pattern at 54° tilt. It can be noted that along the tilt axis **OT**, 110_0, 200_0, 211_0, and 222_0 arcs can be clearly seen while no 310_0 and 321_0 arcs are observed. This observation confirms that the film is indeed [011] textured. Some grains of the film are, however, oriented randomly, as can be seen from the continuous background rings in Figs. 8(b)–(f), of which the intensity ratios follow for those calculated for randomly oriented grains (see Table 3). This is the reason why all the allowed b.c.c. rings are observed in the diffraction pattern at about 0° tilt (Fig. 8a). The 110_1 arc appears at about 20° tilt and splits into two arcs at around 40° tilt (Figs. 8b, c and d). This indicates that the distribution angle, α, of the [011] axis is approximately 10°. The 200_1, 211_1, 211_2 and 211_3 arcs also follow this observation. The α value obtained by the above observation agrees well with the α value, 10°, determined from the $\sin(\omega_0/2)$ *vs* $1/\sin\beta$ plot (Fig. 10).

3.3. *(11$\bar{2}$0)/(001) epitaxy of CoCrTa/Cr film*

This section presents an analysis of the polycrystalline epitaxy between the CoCrTa/Cr bilayer film prepared on a 533 K heated glass substrate (see Table 1). Sputter-deposited $Co_{86}Cr_{12}Ta_2$ films usually have the h.c.p. structure with lattice parameters being very close to those of the pure h.c.p. Co ($a = 2.507$, $c = 4.070$ Å) (Cullity, 1978; Deng, Lambeth & Laughlin, 1993). Cr films obtained by sputtering usually have the b.c.c. structure ($a = 2.885$ Å) (Cullity, 1978). It should be pointed out that the d spacing of the {0002} (0.204 nm), {10$\bar{1}$2} (0.148 nm) and {10$\bar{1}$3} (0.115 nm) planes of the h.c.p. Co are very close to that of the {110} (0.204 nm), {200} (0.144 nm) and {211} (0.118 nm) planes of the b.c.c. Cr. Therefore, the diffraction rings of those planes will be superimposed on or be very close to each other in the diffraction pattern of the randomly oriented Co/Cr bilayer. Fig. 11 shows a bright-field image of the CoCrTa/Cr bilayer at 0° tilt. The Moiré fringes observed in Fig. 11 are due to the overlap of the CoCrTa layer and the Cr layer. The diffraction pattern of the bilayer at 0° tilt is shown in Fig. 12(a). This pattern is typical of the (11$\bar{2}$0) textured Co on (001) textured Cr (Tang, Lu & Thomas, 1995) (note, for $l = 0$ in the hexagonal system; [hki0]*||[hki0]). A very weak CoCrTa 11$\bar{2}$0 ring, which should not appear in the 0° tilt pattern of a [11$\bar{2}$0]* textured film, also appears, indicating the existence of a small fraction of randomly oriented grains. For an h.c.p. CoCrTa film (with the assumption that it has the same lattice parameters as the pure h.c.p. Co), planes of the {10$\bar{1}$0} family have two distinct angles (30 and 90°) with the (11$\bar{2}$0) or [11$\bar{2}$0]* axis (see Table 4 of paper I).

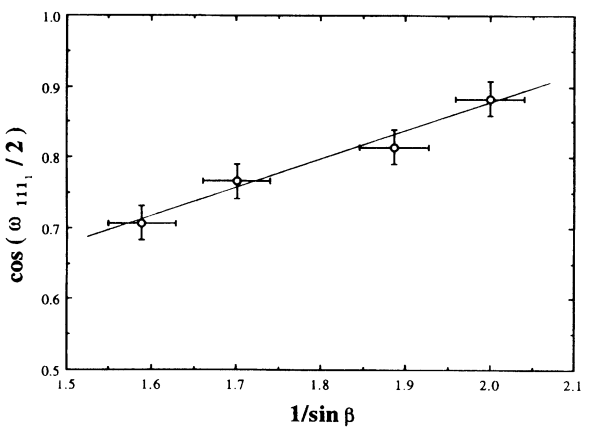

Fig. 5. $\cos(\omega_{111_1}/2)$ *vs* $1/\sin\beta$ plot of the [001] textured MgO film.

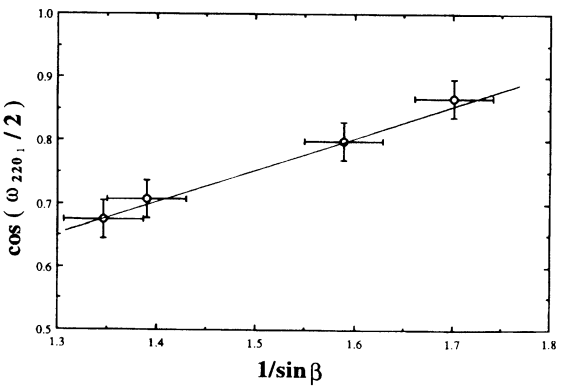

Fig. 6. $\cos(\omega_{220_1}/2)$ *vs* $1/\sin\beta$ plot of the [001] textured MgO film.

Therefore, for a $(11\bar{2}0)$ textured CoCrTa film, the $10\bar{1}0_0$ arcs will appear along the tilt axis when the tilt angle is greater than α and the $10\bar{1}0_1$ arc will appear along the **OF** direction after $60° - \alpha$ of tilt. For diffraction from the planes of the {0002} family, only the 0002_0 arcs are expected to appear along the tilt axis for the $[11\bar{2}0]$* textured film, because there is only one possible angle, namely 90°, between the planes of the {0002} family and the $[11\bar{2}0]$* direction. Planes of the $\{10\bar{1}1\}$ family of the h.c.p. CoCrTa make two distinct angles (39.2 and 90°) with the $[11\bar{2}0]$* axis. Thus the $10\bar{1}1_0$ arc along the tilt axis and the $10\bar{1}1_1$ arc along the **OF** direction will appear after tilting by α and by $49.8° - \alpha$, respectively. The details of the characteristics and the tilt angles needed to observe the various arcs of a [001] textured b.c.c. film can be found in Tang, Lu & Thomas (1995) and Tang & Thomas (1993). Figs. 12(*b*)–(*e*) are the diffraction patterns of the bilayer at 25, 43, 50 and 60° tilt and Fig. 13 is the indexed pattern after a 60° tilt. Along the tilt axis **OT**, arcs of $10\bar{1}0_0$ CoCrTa, 0002_0 CoCrTa/110_0 Cr, $10\bar{1}1_0$ CoCrTa can be clearly seen. No $11\bar{2}0_0$ CoCrTa or 211_0 Cr arcs are observed along the **OT** axis. This observation and the characteristics of the hkl_i arcs in Figs. 12(*b*)–(*e*) and Fig. 13 are consistent with those of the $(11\bar{2}0)$ textured CoCrTa layer on (001) textured Cr layer. The α value determined from the $\sin(\omega_0/2)$ *vs* $1/\sin\beta$ plot (Fig. 14) is 6°.

3.4. *$(10\bar{1}1)$/(011) epitaxy of CoCrTa/Cr film*

We present in this section the results of epitaxy analysis of the CoCrTa/Cr bilayer prepared on a glass substrate heated to 423 K. The bright-field image and the diffraction pattern at 0° tilt of the bilayer are shown in Fig. 15 and Fig. 16(*a*), respectively. Fig. 16(*a*) can be interpreted as the superimposed patterns of the $(10\bar{1}1)$ or $[10\bar{1}1]$* lamellar textured CoCrTa and (011) lamellar textured Cr (note, for h.c.p. films $(10\bar{1}1)$ lamellar texture is not the same as $[10\bar{1}1]$ fibrous texture). The first ring is the 110_0 Cr. The second ring is the 200_0 Cr. The third ring is the $11\bar{2}0_0$ ring of the CoCrTa, which is the only ring that can appear in the parallel pattern for a $(10\bar{1}1)$ textured h.c.p. film. The fourth ring is the 211_0 Cr. Since the diffraction patterns of the (011) textured b.c.c. Cr are the same as those for the (011) textured b.c.c. Ta film except for different texture axis distribution angles, no detailed discussion of the (011) textured Cr film will be given in this section. For a $(10\bar{1}1)$ textured h.c.p. CoCrTa film, since the planes of $\{10\bar{1}0\}$ family have two distinct angles (28.1 and 63.8°) with the $(10\bar{1}1)$ (see Table 4 of paper I), the $10\bar{1}0_1$ and $10\bar{1}0_2$ arcs along the **OF** directions are expected to appear after the film is tilted $26.2° - \alpha$ and $61.9° - \alpha$, respectively. There is only one angle between the {0002} and $(10\bar{1}1)$ planes, which is 61.9°. Thus, the tilt angle needed to observe the 0002_1 arcs is $28.1° - \alpha$. Note that this angle is only 1.9° smaller than that $(30° - \alpha)$ needed to observe the 110_1 arc for a (011) textured b.c.c. Cr film. Because the {110} Cr ($d = 0.20398$ nm) and the {0002} CoCrTa ($d = 0.2035$ nm) have almost identical d spacings, the CoCrTa 0002_1 and the Cr 110_1 arcs will not be distinguishable if α is greater than 1°. Planes of the $\{10\bar{1}1\}$ family have four distinct angles (80.38, 56.2, 52.3 and 0°) with the $(10\bar{1}1)$. Then the $10\bar{1}1_1$, $10\bar{1}1_2$, $10\bar{1}1_3$

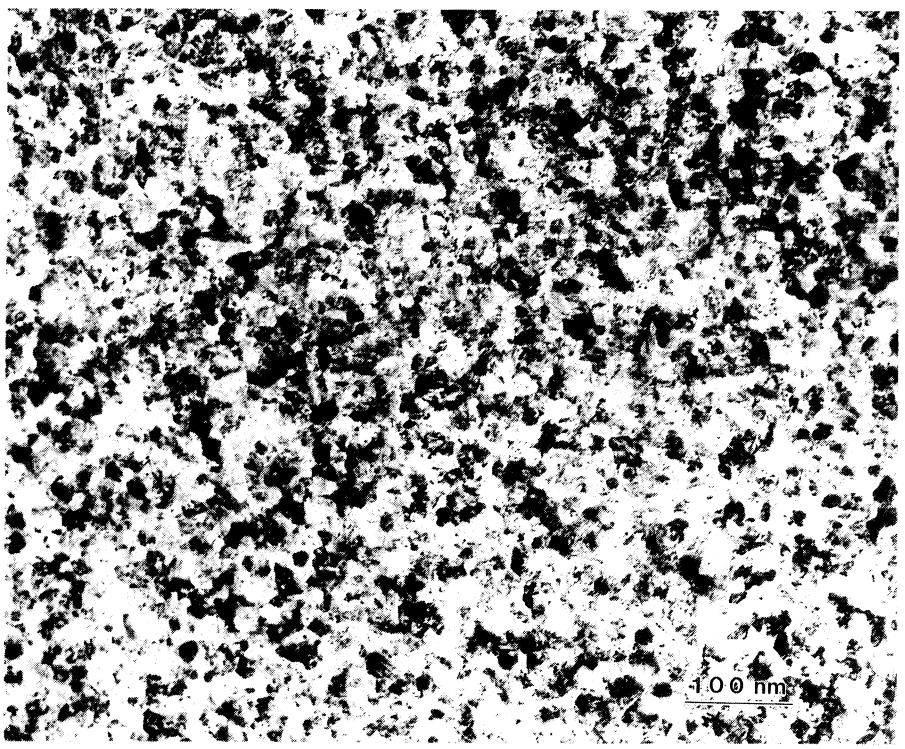

Fig. 7. Bright-field TEM image of the [011] textured b.c.c. Ta film at 0° tilt.

and $10\bar{1}1_4$ arcs will start appearing after tilting to $9.62^\circ - \alpha$, $33.8^\circ - \alpha$, $37.7^\circ - \alpha$, and $90^\circ - \alpha$. It should be noted that if α is greater than 9.62° then the $10\bar{1}1_1$ ring will be present in the parallel pattern and, if α is greater than 2°, the 1011_2 and the 1011_3 arcs are not distinguishable. The diffraction patterns of the bilayer at 10, 30 and 50° tilt are shown in Figs. 16(*b*)–(*d*). Fig. 17 is the indexed diffraction pattern at 50° tilt. These patterns follow well with the above analysis. The $\sin(\omega_0/2)$ *vs* $1/\sin\beta$ plot (Fig. 18) gives the texture axis distribution angle of 6°. Since this angle is smaller than 9.62° and greater than 2°, the CoCrTa 0002_1 arc and the 110_1 Cr arc appear in the patterns as one arc instead of two. The same can be said of the CoCrTa $10\bar{1}1_2$ and $10\bar{1}1_3$ arcs.

4. Conclusions

Texture analysis using diffraction patterns at different tilt angles of an MgO film on an SiO_2 substrate and a Ta film on a glass substrate have been carried out on the basis of the theory developed in paper I (Tang & Laughlin, 1996). The MgO film shows a [001] texture with a distribution angle of 13° and the Ta film shows a [011] texture with a

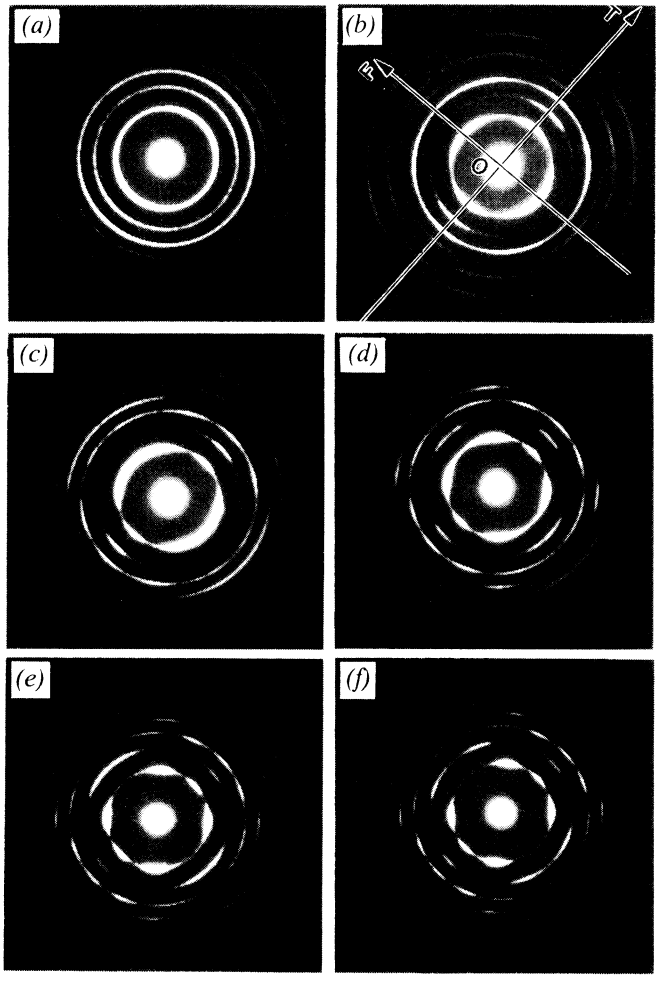

Fig. 8. Electron diffraction patterns of the [011] textured Ta film at (*a*) 0, (*b*) 23, (*c*) 32, (*d*) 38, (*e*) 46 and (*f*) 54° tilt.

Table 3. *Crystallographic parameters and calculated intensity ratios of parallel electron diffraction rings for randomly oriented and [011] textured grains of b.c.c. Ta ($a = 3.303$ Å) films*

hkl	d (Å)	F (Å)	P_r	I_r	$P_{[001]}$	$I_{[001]}$
110	2.34	15.71	6	100	2	100
200	1.65	11.62	3	14	2	27
211	1.35	9.50	12	24	4	24
220	1.17	8.01	6	7	2	7
310	1.04	7.07	12	8	0	0
222	0.95	6.33	4	2	4	5
321	0.88	5.75	24	8	0	0

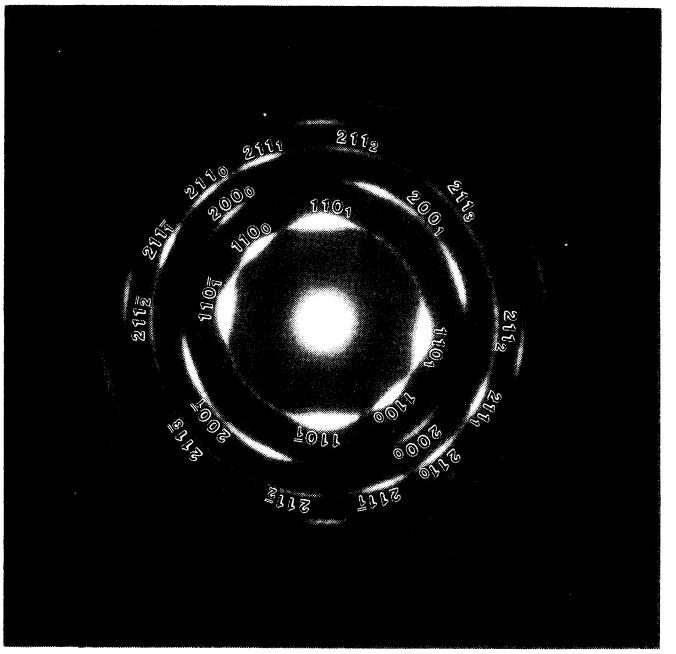

Fig. 9. Indexed electron diffraction pattern of the [011] textured Ta film at 54° tilt.

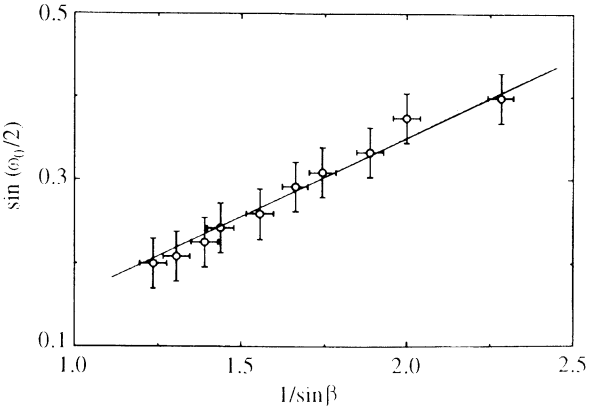

Fig. 10. $\sin(\omega_0/2)$ *vs* $1/\sin\beta$ plot of the [011] textured Ta film.

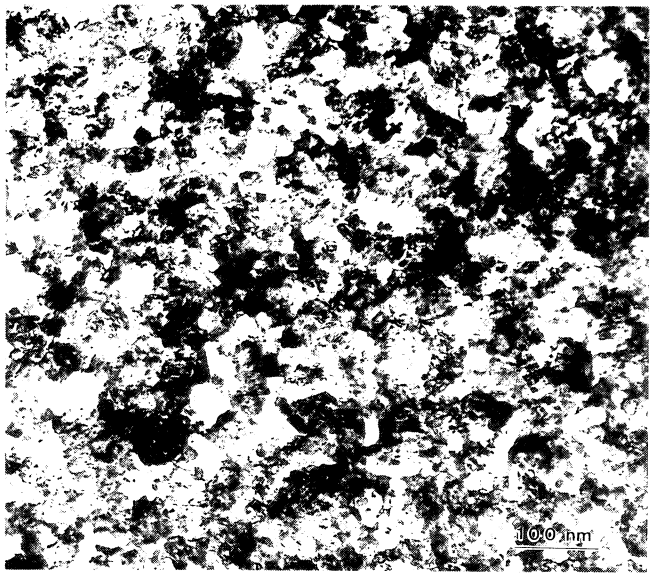

Fig. 11. Bright-field TEM image of the $(11\bar{2}0)$CoCrTa/(002)Cr bilayer film at 0° tilt.

Fig. 13. Indexed electron diffraction pattern of the $(11\bar{2}0)$CoCrTa/(002)Cr bilayer film at 60° tilt.

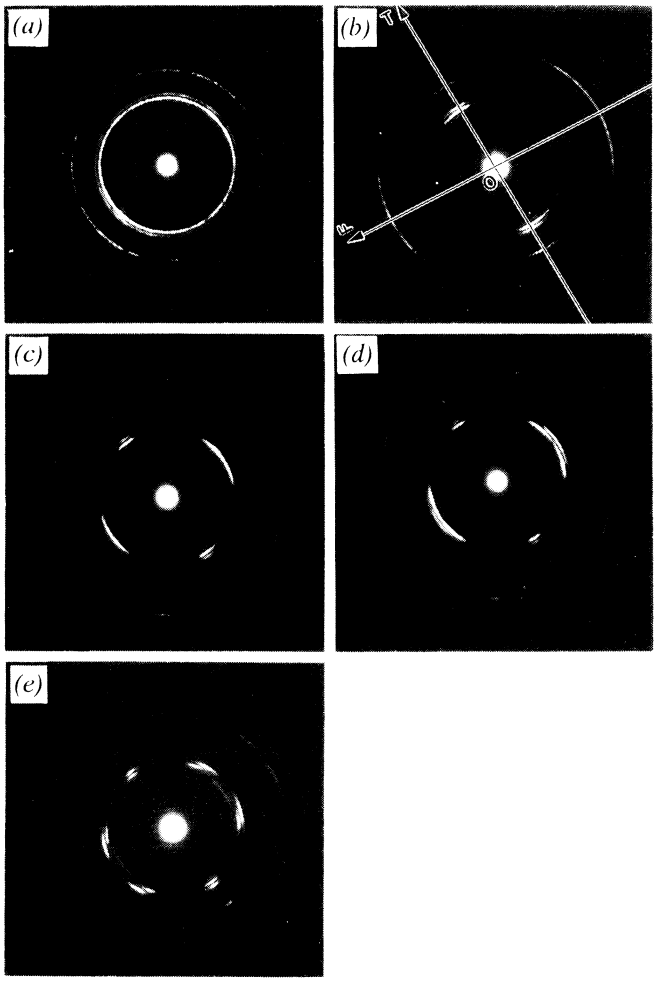

Fig. 12. Electron diffraction patterns of the $(11\bar{2}0)$CoCrTa/(002)Cr bilayer film at (*a*) 0, (*b*) 25, (*c*) 43, (*d*) 50 and (*e*) 60° tilt.

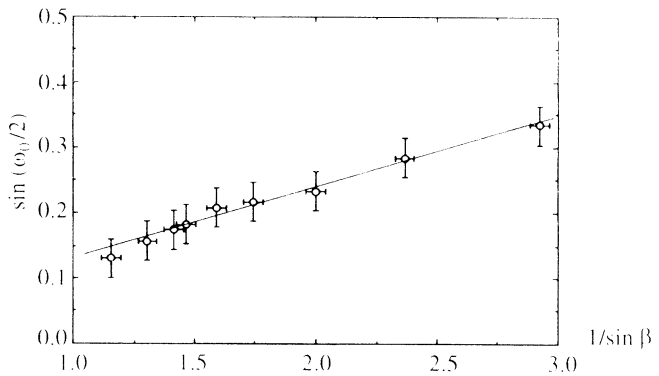

Fig. 14. $\sin(\omega_0/2)$ *vs* $1/\sin\beta$ plot of the $(11\bar{2}0)$CoCrTa/(002)Cr bilayer film.

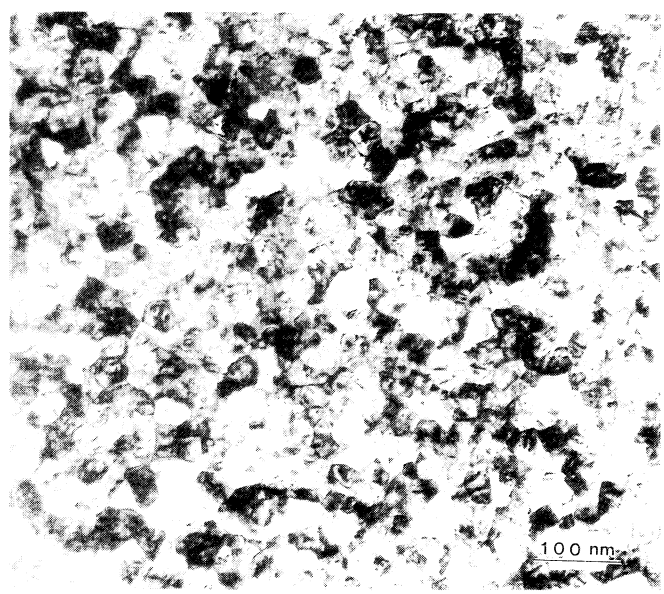

Fig. 15. Bright-field TEM image of the $(10\bar{1}1)$CoCrTa/(011)Cr bilayer film at 0° tilt.

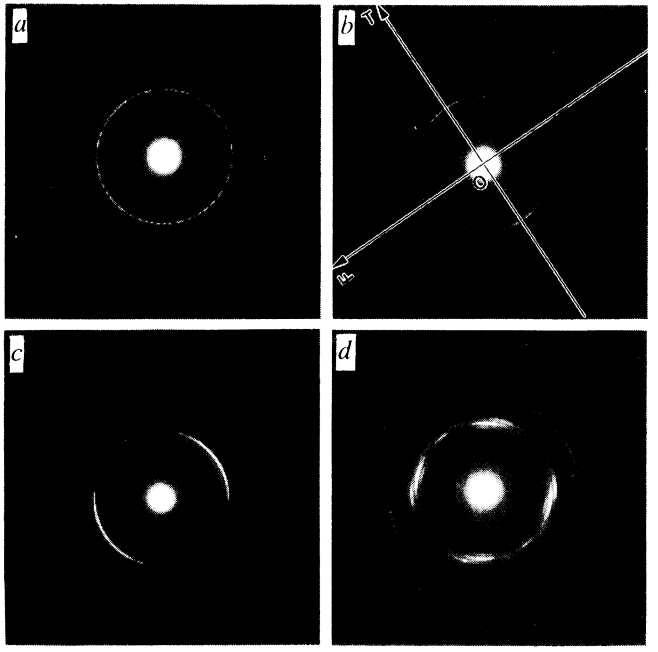

Fig. 16. Electron diffraction patterns of the $(10\bar{1}1)$CoCrTa/(011)Cr bilayer film at (*a*) 0, (*b*) 10, (*c*) 30 and (*d*) 50° tilt.

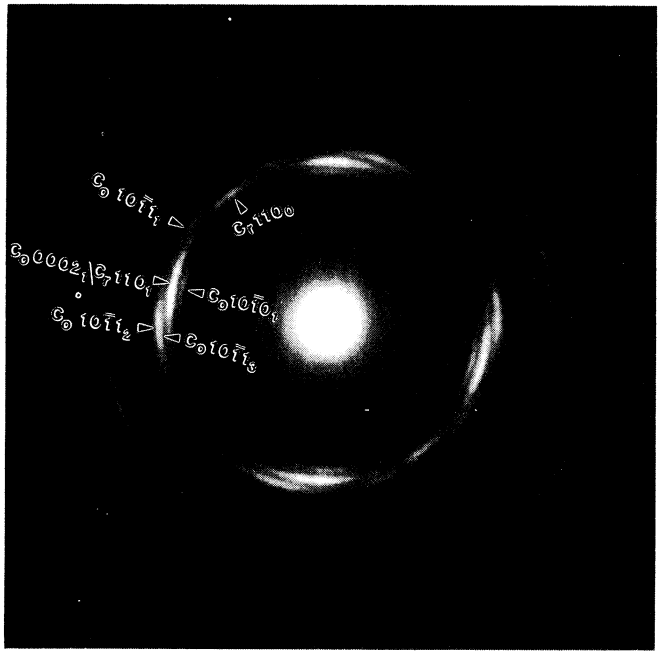

Fig. 17. Indexed electron diffraction pattern of the $(10\bar{1}1)$CoCrTa/(011)Cr bilayer film at 50° tilt.

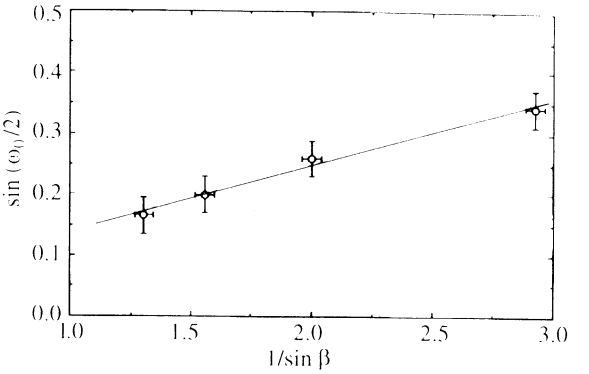

Fig. 18. $\sin(\omega_0/2)$ *vs* $1/\sin\beta$ plot of the $(10\bar{1}1)$CoCrTa/(011)Cr bilayer film.

distribution angle of 10°. Diffraction patterns at different tilt angles of $(11\bar{2}0)$CoCrTa/(001)Cr and $(10\bar{1}1)$CoCrTa/(011)Cr bilayer films on glass substrates have also been presented and discussed. Both of these bilayer films have a texture axis distribution angle of about 6°. Experimental observations of the diffraction patterns at different tilt angles agree well with the theoretical analysis.

The authors thank Professor M. De Graef of Carnegie Mellon University for his critical reading of the manuscript. This work is supported by the National Science Foundation under grant ECD-8907068. The US government has certain rights to this material.

References

Cullity, B. D. (1978). *Elements of X-ray Diffraction*, p. 506. Reading, MA: Addison Wesley.

Deng, Y., Lambeth, D. N. & Laughlin, D. E. (1993). *IEEE Trans. Magn.* **29**, 3676–3678.

JCPDS Diffraction Data Card (1992). ICDD No. 4-829. JCPDS (now International Centre for Diffraction Data), 1601 Park Lane, Swarthmore, Pennsylvania, USA.

Read, M. H. & Altman, C. (1965). *Appl. Phys. Lett.* **7**, 51– 52.

Read, M. H. & Hensler, D. H. (1972). *Thin Solid Films*, **10**, 123–135.

Tang, L. & Laughlin, D. E. (1996). *J. Appl. Cryst.* **29**, 411–418.

Tang, L. & Thomas, G. (1993). *J. Appl. Phys.* **74**, 5025–5032.

Tang, L., Lu, D. & Thomas, G. (1995). *J. Appl. Phys.* **77**, 47–53.